Cell Membranes Open "Doors" for Cationic Nanoparticles/Biomolecules: Insights into Uptake Kinetics

Jiaqi Lin and Alfredo Alexander-Katz*

Department of Material Science and Engineering, Massachusetts Institute of Technology, Cambridge, Massachusetts 02139, United States. All authors conceived and designed the project; J.L. performed the simulations. All authors analyzed, interpreted the data, and wrote the manuscript.

ABSTRACT Cationic nanoparticles (NPs) and cell-penetrating peptides (CPPs) can enter cells in an energy-independent fashion, escaping the traditional endocytosis route, which is known as direct translocation. This unconventional entry, usually complementary to endocytosis, features rapid uptake and thus makes both cationic NPs and CPPs fascinating intracellular delivery agents. However, the mechanisms of the direct translocation of both cationic NPs and CPPs across cell membranes into the cytosol are not understood. Moreover, the relationship between direct translocation and endocytosis is also unclear. Here, using coarse-grained molecular dynamics simulations we show that a model cell membrane generates a nanoscale hole to assist the spontaneous translocation of cationic gold nanoparticles (AuNPs) as well as HIV-1 Tat peptides to the cytoplasm side under a transmembrane (TM) potential. After translocation, the AuNPs/Tat peptides move freely in the "cytoplasm" region and the membrane reseals itself within a microsecond, while the TM potential is strongly diminished. Furthermore, we show that the shape of the cationic object is crucial in determining if it can translocate or not across. The results provide insights into the uptake kinetics of cationic NPs/CPPs, which features the relationship between direction translocation and endocytosis. The mechanism put forward here establishes fundamental principles of the intracellular delivery of cationic nanocarriers.

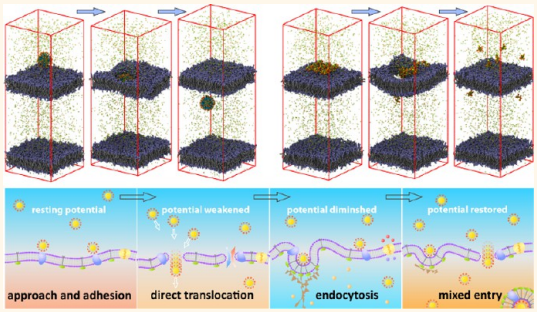

KEYWORDS: cell membranes · nanoscale holes · gold nanoparticles · cell-penetrating peptides · direct translocation · transmembrane potential

The living cell plasma membrane serves as a boundary that regulates the import and export of molecules. Ions and small molecules enter cells by passively diffusing across lipid bilayers or through membrane channels. Large solid objects enter cells by a mechanism called endocytosis, during which the cell membrane engulfs the objects into membrane-bound vesicles and directs them to designated intracellular pathways.[1] Recently, it was discovered that cationic nanoparticles (NPs) are able to enter cells in a nonendocytotic fashion,[2] featuring fast and large uptake, without toxic effects to the cell if introduced at low concentration.[3] These properties make cationic NPs promising candidates for drug delivery.[4,5] On the other hand, scientists discovered that certain proteins possess short sequence segments that manage to make the proteins translocate across cell membranes in a seemingly energy-independent manner.[6] These small segments, which are named cell-penetrating peptides (CPPs), are positively charged and proven exceptionally effective in delivering cargos of various sizes (from small chemical molecules to large fragments of DNA) into cells.[7−9] Although both cationic NPs and CPPs have shown great potential as drug transporters, the mechanism by which they translocate across cell membranes into cells is yet unclear.

Experiments with cationic AuNPs show that their uptake is extremely fast (within seconds) and is ATP-independent (at 4 °C).[3] Upon entry to cells, these NPs can induce depolarization as well as the increase of Ca^{2+} level in the cytosol. However, prior depolarization of the cells can lead to a large reduction in uptake. Patch clamp studies show an unregulated current−voltage relationship, implying that nanoscale disruption may be generated on membranes.[10] It is also reported that cationic NPs can generate defects or expand pre-existing

* Address correspondence to aalexand@mit.edu.

Received for review August 4, 2013 and accepted November 19, 2013.

Published online November 19, 2013
10.1021/nn4040553

defects on supported lipid bilayers due to strong binding between the particles and the lipids.[11] However TEM studies have failed to observe direct evidence of membrane disruption in living cells.[3] Although it is believed that "holes" or "pores" are generated on the cell membrane to assist the NP's entry, the exact mechanism of translocation is unknown.[12] For CPPs, a diverse set of experiments show that there might be more than one pathway responsible for their uptake.[8] A mixed type of endocytosis happens at low concentration, while energy-independent translocation takes place at high concentration, with CPPs dispersed in the cytosol.[13,14] The uptake of cationic CPPs also strongly depends on the transmembrane (TM) potential.[15] There are several existing hypotheses pertaining to the spontaneous translocation of CPPs, such as the inverse micelle model,[16] the carpet model,[17] and the barrel-stave model.[18] However, these models do not provide a satisfactory explanation of the exact translocation process.

Meanwhile, extensive simulation studies have emerged in an attempt to capture the mechanism of energy-independent translocation behavior of cationic NPs and CPPs. Generally it is found that cationic NPs absorb or bind strongly to lipid bilayers, causing deformation of the membrane in favor of endocytosis.[19−21] On the other hand, simulation of CPPs shows that they can migrate across the hydrophobic interior of the lipid bilayer due to strong attraction between the peptides and the phosphate groups on both sides of the bilayer.[22] Although these results capture the strong interaction of cationic NPs and CPPs with lipid membranes, they fail to explain how these particles translocate across membranes freely to the other side and disperse into the cytosol, as experiments clearly show that NPs/CPPs are inside the cell cytoplasm.[2,13]

Considering the similarity between cationic NPs and CPPs (both are positively charged) and the connection between their translocation pathways across cell membranes (energy-independent, concentration-dependent, extremely fast, transmembrane potential triggered), one may ask a question: can they share the same translocation mechanism? Here we attempt to answer this question.

For nanoparticle−membrane simulation, viable methods are all-atomic molecular dynamics (AA MD), coarse-grained molecular dynamics (CG MD), dissipative particle dynamics (DPD), and self-consistent field theory (SCFT), *etc*.[23] AA MD gives many molecular details but has limited time and length access. DPD proves powerful in modeling large membrane deformations such as endocytosis,[21,24] but it uses a soft potential, which does not include charge and dipole interactions. SCFT focuses on the thermodynamics, which proves useful in describing membrane morphology[25] but not charged interactions. Therefore, the most suitable method to describe the system we are interested in is CG MD with proper electrostatic interactions. Here we use the "MARTINI" CG force fields[26] with explicit polarizable water solvent,[27] which gives a relative realistic description of the charge and dipole interactions of the membrane system.[24] Construction of AuNPs and the Tat peptide model compatible with the MARTINI CG force field is fully described in the Supporting Information. The AuNP has a core diameter of 2.2 nm and is covered by 104 dodecane ligands with their terminus functionalized with an ammoniate group. The HIV-1 Tat peptide has the residues YGRKKRRQRRR, which features positively charged arginine and lysine (Figure 1a). Full details of the CG model and construction of the nanoparticle and peptides can be found in the Supporting Information. To model a TM potential under periodic boundary conditions, a double dipalmitoylphosphatidylcholine (DPPC) bilayer system is built, dividing the system into two regions: an "extracellular" region, which has a relatively negative potential, and an "intracellular" region, which has a relatively positive potential. Salt (NaCl) is introduced to the solvent at the physiological concentration (150 mM). The TM potential is generated by imposing charge imbalance between these two regions (extra Na^+ in "extracellular" region and extra Cl^- in "intracellular" region). In our system size (18 nm × 18 nm × 50 nm), one charge imbalance creates approximately −0.04 V TM potential (Figure 1b). A larger membrane with the same charge imbalance density per area of lipid, however, generates a smaller TM potential due to membrane undulations.

RESULTS AND DISCUSSION

Translocation of NPs. To test the internalization pathway of cationic nanoparticles, a cationic AuNP was placed 3 nm above the surface of the upper bilayer in the double-membrane system with −1.5 V TM potential (30 ionic imbalances) as initial configuration of the simulation. During the dynamics run, the AuNP directly translocated across the upper bilayer to the "intracellular region", as is shown by Figure 2a in perspective view (see SV1 for full trajectory). Figure 2b shows 2.2 nm cationic AuNPs (0.4 μM) inside the cytosol of human bronchial epithelial cells without endosomes, indicating a nonendocytotic entry,[2] which is consistent with our simulation. Figure 2c gives the details of the translocation process. Initially, the AuNP and membranes were constrained for 10 ns to equilibrate water and ions. After releasing the constraints, the upper membrane immediately showed a large deformation and a hole started to form near the center of the membrane. On the other hand, the AuNP started to move toward the hole. As the nanoparticle reached the entrance of the hole, it moved straight downward to pass through the hole. After exiting the hole, the AuNP continued to move down and diffuse freely in the "intracellular region". The entire penetration process takes about 40 ns. After the AuNP translocated to the other side, the bilayer recovered from deformation and the hole began to close. At roughly 60 ns, the hole was completely resealed, resulting in a neat bilayer like its initial state.

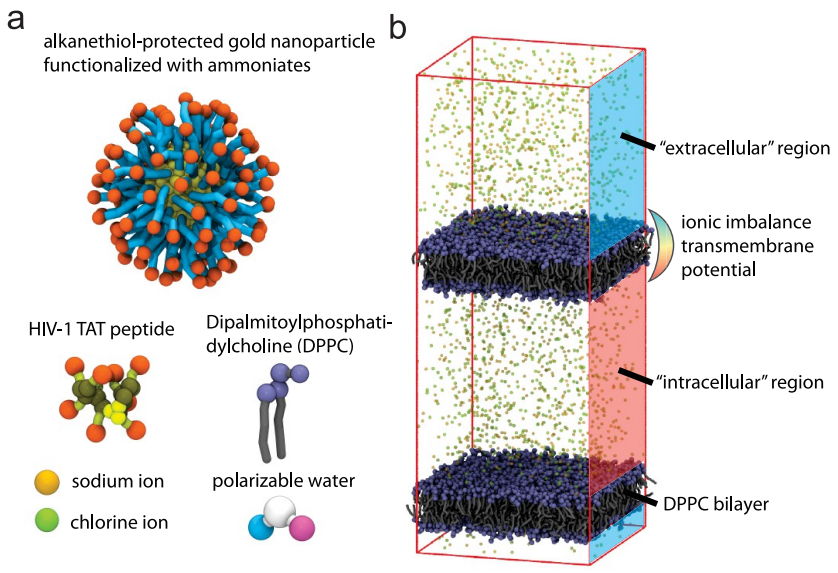

Figure 1. (a) Illustration of the individual components used in the simulation. Polarizable water has two lateral CG beads, which carry a positive and a negative charge, respectively. (b) The double membrane system with a transmembrane (TM) potential. The "intracellular" region has *X* more Cl^- and *X* less Na^+ than the "extracellular" region, which results in a TM potential of $-(0.04X)$ V.

Figure 2d shows the area of the hole opened on the upper membranes as a function of simulation time. The hole started to form 2 ns after adding the AuNP to the system, and it expanded rapidly to its maximum size, around 28 nm^2, at 15 ns. Then the size of the hole quickly dropped down to about 3 nm^2, and afterward it gradually decreased to zero.

Figure 2e gives the ionic current of Na^+ and Cl^- passing through the hole as a function of simulation time. At the initial stage of hole formation, a large amount of Na^+ current flowed inward, while the same amount of Cl^- flowed outward, to rebalance the TM potential across the membranes. At around 15 ns, when the AuNP was just penetrating the hole, another surge of Cl^- current flowed inward. This is because the surface of the AuNP is covered with chlorine ions, which were carried with the particle across the bilayer. A recent experiment shows that a noncytotoxic concentration of cationic nanoparticles induces currents from 30 to 3000 pA in human embryonic kidney and epidermoid carcinoma cells.[10] The magnitude of the current in the simulation here agrees with experimental measurements. Generally, a hydrophilic transmembrane pore is generated by the stress exerted on the bilayer membrane. When the stress is removed, the membrane will return to its natural state, which is a perfect bilayer. In this case, the uneven distribution of charges causes the formation of a hydrophilic pore on the upper membrane. After the translocation of the AuNPs as well as the exchange of ions, the charges are evenly distributed across the membrane, which allows the bilayer to relax and consequently to reseal the pore. Realistically, pores on living cell membranes can only reseal themselves when mechanical stress on the membrane is removed as well as local transmembrane potential around the pores disappears.

Figure 2f gives the TM potential as a function of distance along the bilayer normal at three different stages of the simulation. The pure bilayer system without AuNPs has a TM potential of ~1.5 V. When the AuNP was added to the system and constrained to the initial position, the TM potential surged to approximately −4 V, which results in a transmembrane electric field up to −0.5 V/nm. It was reported that such high electric field was enough to induce electroporation on pure lipid bilayers.[28] Cell membranes, however, are embedded with various proteins, which typically possess higher polarities compared to the hydrophobic lipid tails. This may significantly reduce the local TM potential required to generate holes on the cell membrane. It should be noted that the potential gradient is not felt by the nanoparticle at this moment, implying that a hole must be created prior to the AuNP's downward movement. Finally, after the AuNP translocation and the exchange of ions across the bilayer, and the subsequent closure of the hole, the TM potential is reduced to a minor value of +0.1 V, suggesting that this hole-generating translocation mechanism can cause depolarization of cells. Indeed, recent experiments show that cationic AuNPs are able to reduce the TM potential of up to 60 mV in four different cell lines.[3]

Figure 3 gives the electric potential profile of the system when the hole was at its fastest expanding rate and the AuNP was about to penetrate the hole at 4 ns. The potential profile was generated using 20 frames with an interval of 0.02 ns. Five two-dimesional potential contour maps corresponding to slices at different *x* coordinates (the yellow planes in the perspective box)

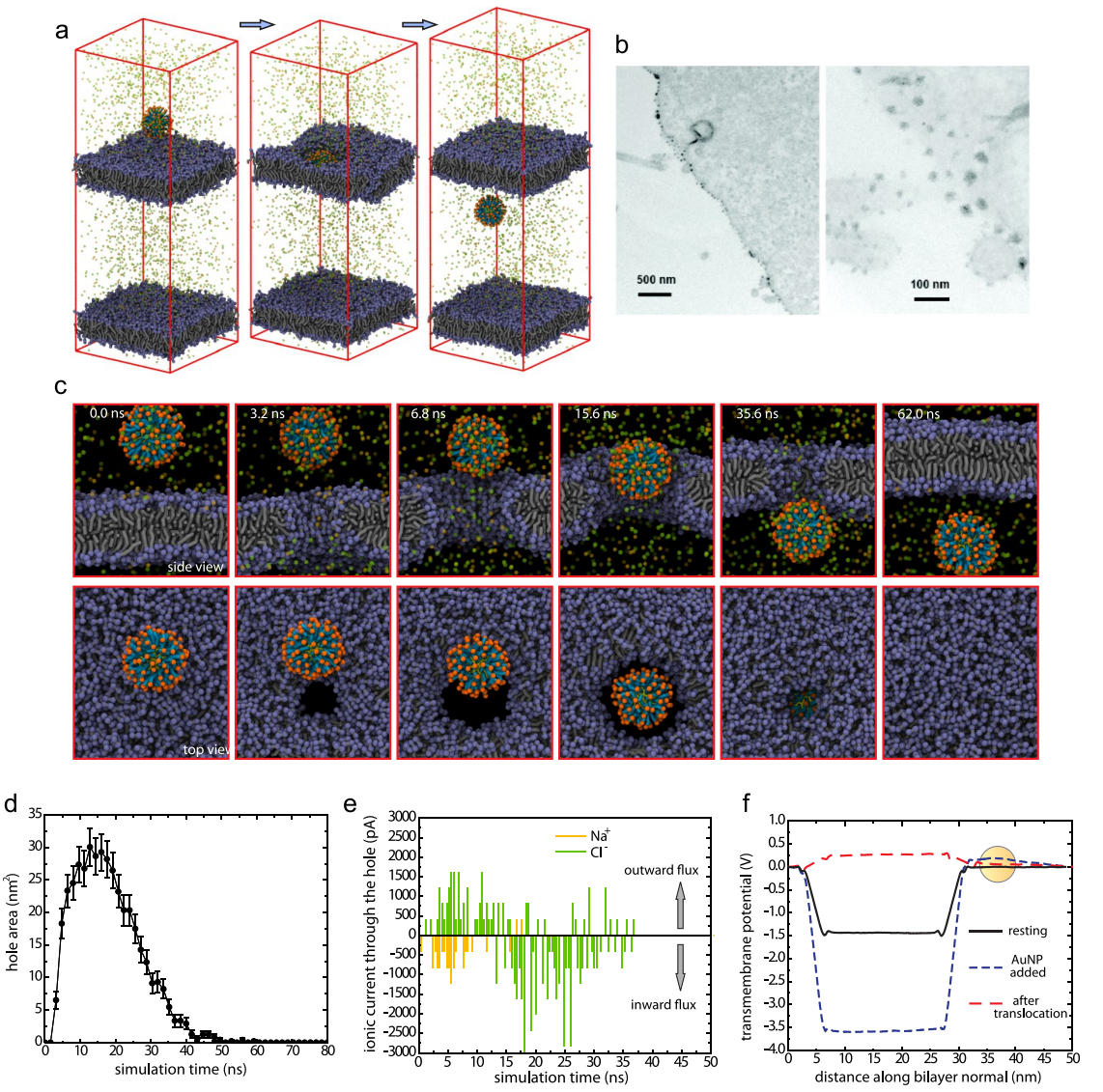

Figure 2. Direct translocation of a cationic AuNP across a lipid membrane under −1.5 V TM potential. (a) Perspective view of the AuNP−double-bilayer system at the beginning of the simulation, the AuNP penetrating through the hole, and the end of the simulation. (b) TEM image indicating nonendocytotic uptake of cationic AuNP (concentration = 0.4 μM) in human bronchial epithelial cells without disrupting the cell plasma membrane.[3] (c) Snapshots of the side view and top view of the penetration process. Ions and water are omitted in the top view for clarity. (d) Area of the hole generated on the upper membrane as a function of simulation time. Error bars indicate standard error of the mean (SEM). (e) Na^+ and Cl^- current flow through the hole as a function of simulation time. (f) TM potential at different stages of simulation: double-membrane system resting, initial addition of AuNP, and the end of simulation after AuNP translocation and membrane reseal.

are given. Profiles 1, 2, and 3 cut through the hole, while profiles 2, 3, and 4 cut through the nanoparticle. Profile 5 cuts through the normal region on the bilayer membrane without touching the AuNP or the hole, where the potential difference between "extracellular region" and "intracellular region" is mostly maintained. As it comes closer to the "hole" region, the difference of potential between the two regions is gradually compromised. Note that in profile 1, which cuts through the center of the hole, the potential difference around the hole disappears, while it slightly remains at the periphery regions. The AuNP features a highly positive potential, which can be easily identified in profiles 2, 3, and 4 as a red ball. Profile 2 shows that a small continuous potential gradient exists between the AuNP and the intracellular region, as the color transition from red to blue through the hole. This potential difference results in the driving force that drags the AuNP downward through the hole, which is the direct reason for the nanoparticle translocation. Stationary ions can also be clearly identified in all the profiles, as they gather on the surface of both upper and lower membranes. Profile 2 shows that the rim of the hole is also covered by Na^+ and Cl^-. These ions may exert collective forces on the membrane that contribute to the deformation of the membrane and the generation of the hole.

To prove that the TM potential is responsible for the cationic nanoparticle translocation, simulations were

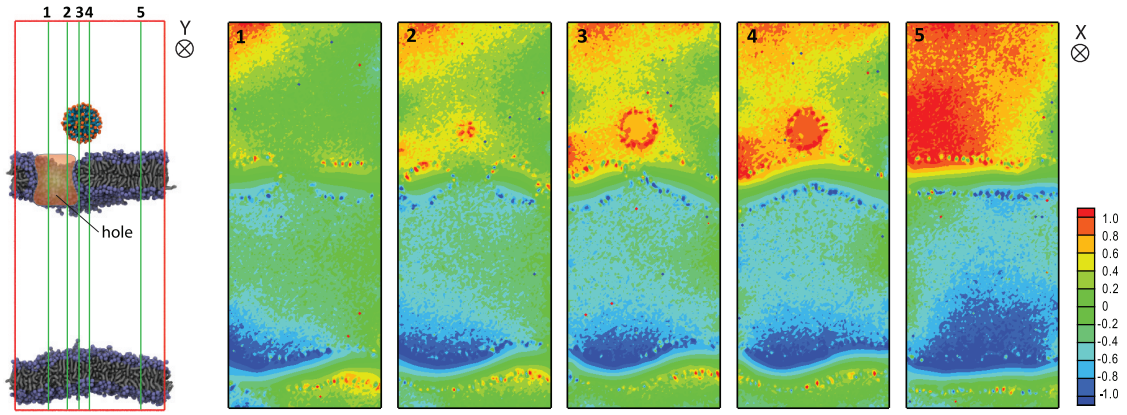

Figure 3. Potential contour maps of the double-membrane system when the AuNP is dragged toward the hole 4 ns after its release. Each contour map corresponds to each cross sectional slice at different *x* coordinates in the perspective snapshot (1, 2, 3, 4, and 5). The potential in the contour maps is in volts.

carried out with zero TM potential. In this case, neither hole formation nor nanoparticle translocation was observed after introducing the AuNP to the double-membrane system. Instead, the AuNP was found to attach to the surface of the upper membrane, consistent with previous simulations.[20] Experiments show that the uptake of cationic AuNPs in depolarized cells (treated with 40 mM KCl) is significantly reduced compared to that in normal cells, which further corroborates that the TM potential is a major factor in causing nonendocytotic translocation. In the case of anionic AuNPs, the simulation revealed that they do not induce hole formation under TM potential, and therefore no translocation occurs. Instead they also attach to the bilayer surface, implying an endocytotic entry or other energy-independent pathway that is still not clearly understood.[29]

For the case where the TM potential is low, approximately less than or equal to 0.2 V (5 ionic imbalances), a single cationic AuNP binds only to the upper surface of the membrane (the second configuration from left), a common motif for charged nanoparticles found in various simulations.[20] A recent experiment shows that cationic AuNPs penetrate DSPC (1,2-distearoyl-*sn*-glycero-3-phosphocholine) floating lipid bilayers and reside in the hydrophobic moiety.[30] Without a TM potential, such insertion is indeed energetically favorable but is difficult to observe in simulations since it takes seconds for the nanoparticle to overcome the water–bilayer interface.[31] In this case, one NP is not enough to generate holes, but it does exert stress on the membrane, resulting in bilayer stretching. A 12.2% increase in area is observed. Such stresses could lead to large undulations in living cell plasma membranes.[3] We then introduced a second AuNP 15 nm above the upper surface of the membrane. After the insertion of the second AuNP, hole formation occurred on the upper membrane beneath the first AuNP, and it subsequently translocated across the bilayer. The second AuNP was not able to translocate to the "intracellular region", as the hole was closed before it could reach the proximity of the membrane. This result suggests that a higher concentration of cationic nanoparticles is more likely to break cell membranes and allow them to translocate across it. Indeed, experiments have shown that a higher concentration of AuNPs can cause a larger change to the TM potential.[3] Furthermore, in the simulations that have two AuNPs, only the AuNP closer to the membrane will translocate, while experiments have shown that half of the cationic AuNPs enter cells through direct translocation while the other half is subject to energy-dependent entry.[3,32] Simulations show that nanoparticles closer to cell membranes or already attached to their surface seem more likely to translocate.

Translocation of CPPs. During the past decades, the cell entry of CPPs was the subject of strong controversy. Several mechanisms including the inverse micelle model and the membrane disruption model (with peptide migration) were proposed regarding the mechanism of CPPs' energy-independent entry. Our simulations, however, suggest a TM potential-driven membrane-hole assisting entry mechanism that differs from the existing ones. To test the translocation behavior of CPPs, an HIV-1 Tat peptide was put 3 nm above the upper membrane under −1.5 V TM potential, as in the case of AuNP. Here a single Tat peptide carries 8 positive charges, while an AuNP carries 104 positive charges. For the case of one Tat peptide, it eventually attached to the membrane surface without generating holes. To increase the concentration we put nine Tat peptides above the upper membrane in a plane normal to the *z*-axis (Figure 5a). The charge that they carried in total was comparable to that of the AuNPs investigated before. Similarly, when the peptides are released after equilibration, the membrane experienced large deformation and a hole was formed beneath the peptides but slightly displaced. As the hole was formed, four of the peptides closer to the aperture were sucked into the hole and consequently translocated across the bilayer (Figure 5c and SV2).

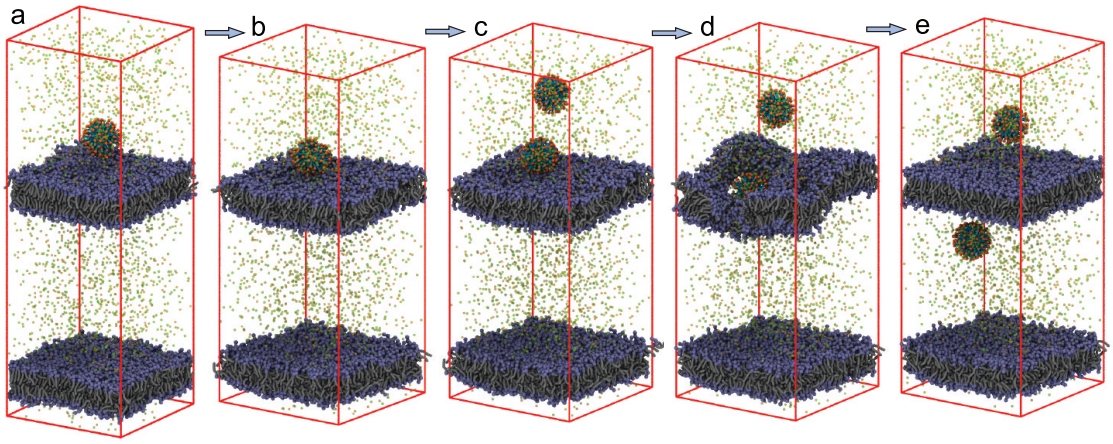

Figure 4. Direct translocation of AuNPs across lipid membranes under a −0.2 V TM potential. (a) Initial setup of the simulation. (b) AuNP attached to the surface of the membrane. Snapshot is taken at the end of the 120 ns simulation. (c) A second AuNP was introduced 15 nm above the upper membrane in the "extracellular region". (d) A hole formed on the upper membrane and the first AuNP penetrated though the hole. (e) The first AuNP completely translocated into the "intracellular region", while the second AuNP remained at the "extracellular" region, and the membrane resealed itself. Snapshot is taken at 280 ns of the simulation.

After translocation, those four peptides moved freely in the "intercellular region" and the hole resealed itself at roughly 60 ns. The area of hole as a function of time shows a similar trend to that for AuNP, only with a smaller value and a longer initial time before its formation (Figure 5d). As we reduced the number of the peptides to five or lower, the formation of holes on the bilayer membrane and their translocation was not observed, suggesting their entry into the cell is concentration-dependent (Figure S7). Again, the concentration dependence of HIV-1 Tat peptides' translocation is reported in many experiments.[6,13,14]

Figure 5b shows the cellular uptake of the Tat peptide in a HeLa cell using fluorescence at different concentrations (5, 10, and 20 μM, respectively).[13] At 5 and 10 μM, the Tat peptide was found only in vesicles, implying an endocytotic entry, which is consistent with our simulations, where peptides attach to the membrane surface only at low concentration (Figure S7). In contrast, Tat peptides at 20 μM are found evenly distributed in the cytosol in most of the cells, indicating direct entry. This corresponds to our simulation of peptides translocating across cellular bilayer membranes at high concentration. Similar to nanoparticles, experiments show that direct translocation is always supplemented by endocytosis, which agrees with our simulation results that nearly half of the CPP does not translocate. In a lipid vesicle assay, it is found that penetratin and its related peptides translocate across lipid bilayers only in the presence of a transbilayer potential,[33] and they induce minimal perturbation to the overall integrity of the bilayer, which further corroborates our simulation results.

The above simulation utilizes nine separate peptides. This lends the question, What if we combine these peptides together and give them a structure? Bearing this in mind, we constructed a compact cluster (Figure 6a) and a long peptide chain (Figure 6b) with its secondary structure as an α-helix using these nine peptides. As we put them in the same simulation, the observed result is quite different. For the compacted cluster, it penetrates through the hole as the AuNP did (Figure 6c). For the α-helix, it does not translocate across the membrane, although a hole was generated on the bilayer (Figure 6d). This indicates that different molecular shapes could result in completely different cell entry mechanisms.

Since the living biological membranes are slightly negatively charged, we introduced negative lipids, DPPG (dipalmitoylphosphatidylglycerol), to the DPPC bilayer. Two kinds of negative bilayer (10% DPPG and 20% DPPG) have been tested. For both negative bilayers, results show that AuNPs and CPPs translocated across the "intracellular region" through holes generated on the membrane with little change to the pure DPPC bilayer. These negative lipids seem to have little effect on the translocation behavior of both AuNPs/CPPs, as the excessive negative charges may be screened by the counterions. A notable earlier work involves a series of simulations carried out by H. Lee and R. Larson[34] to study dendrimer−membrane interactions using the standard MARTINI CG force field (without polarizable water). The results show that cationic dendrimers generally bind to a bilayer membrane surface, while larger dendrimers may induce holes on the bilayer. However, holes induced by cationic dendrimers involve strong binding between its NH_3^+ terminals and lipid head groups, which follows a different mechanism of hole generation under transmembrane potential here. Interestingly they found that a relative spheroidal shape of the dendrimer is

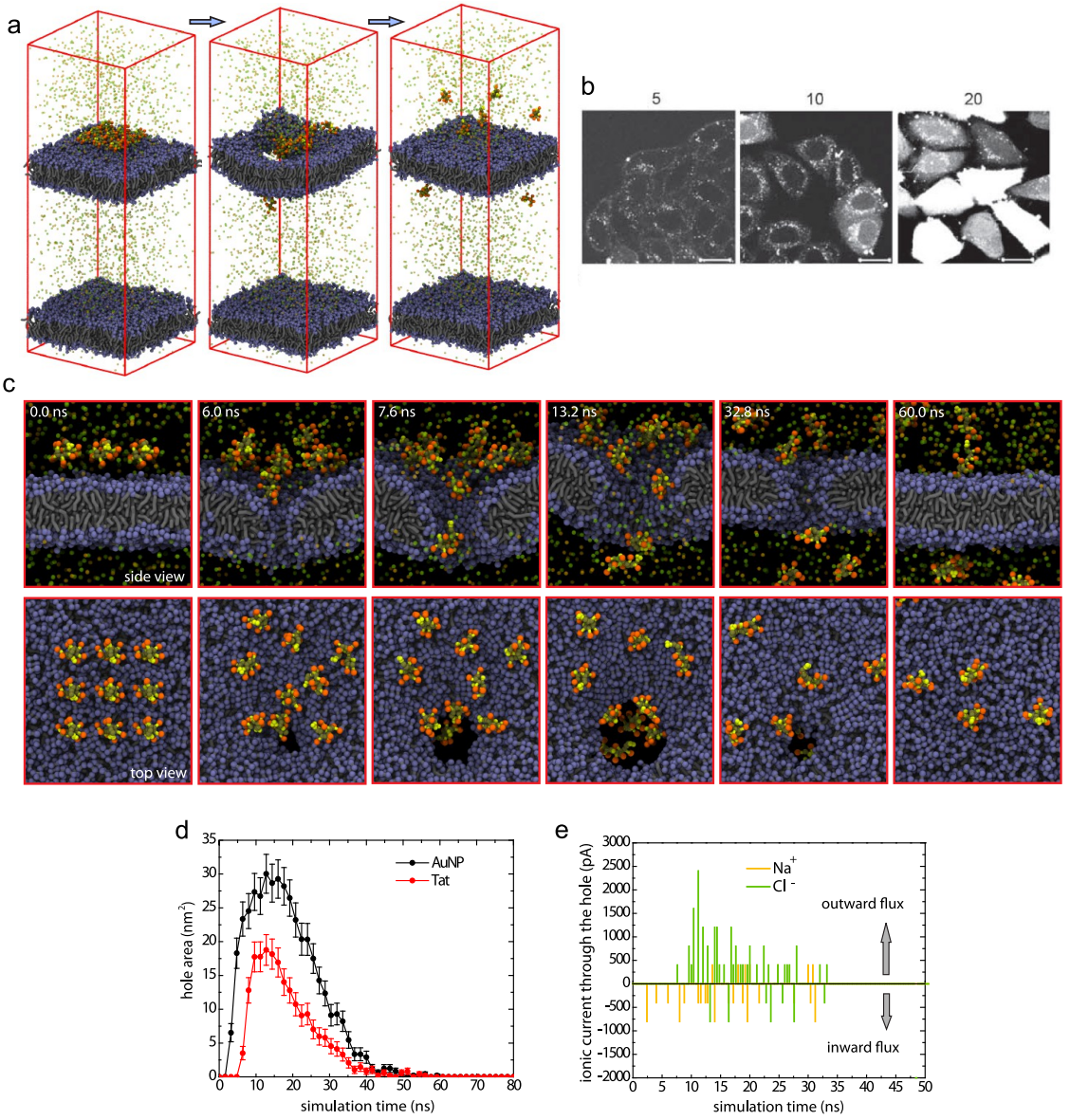

Figure 5. Direct translocation of HIV-1 Tat peptides across a lipid membrane under −1.5 V TM potential. (a) Perspective view of the 9-peptide−double-membrane system at the beginning of the simulation, Tat peptides penetrating through a hole, and the end of the simulation. (b) Uptake of Tat peptides in HeLa cells at different concentration (5, 10, and 20 μM; scale bar is 20 μm).[13] (c) Snapshots of side view and top view of the penetration process. Ions are omitted in the top view for clarity. (d) Area of the hole generated on the upper membrane by Tat peptide and AuNP as a function of simulation time, respectively. Error bars indicate SEM. (e) Na^+ and Cl^- current through the hole as a function of simulation time.

more efficient than a linear shape of poly-L-lysine polymer in increasing membrane permeability,[35] which seems to some extent to agree with our simulation that showed that clustered peptides are more likely to translocate compared to linear peptides.

Uptake Kinetics. The results allow us to gain an in-depth look into the intracellular uptake kinetics of cationic nanoparticles/biomolecules. When a certain concentration of cationic nanoparticles/biomolecules is added to the extracellular medium, a small portion of the cationic particles reaches the cell membranes by diffusion. Once they come close to the membranes, these particles are attracted to the charged membrane proteins located on the cell surface (Figure 7a). As more cationic particles diffuse closer to the membrane, they begin to alter the local electric field across the membrane. When a certain concentration of particles is reached in the local membrane area, holes begin to open on the membranes, which provide passage for direct translocation of the particles that are already attached to the membrane surface (Figure 7b). The fast direct translocation corresponds to the initial surge of uptake of cationic AuNPs.[32] However the hole-opening direct translocation weakens the transmembrane potential of the targeted cells. As more holes are opened on the membrane, at a certain point, the

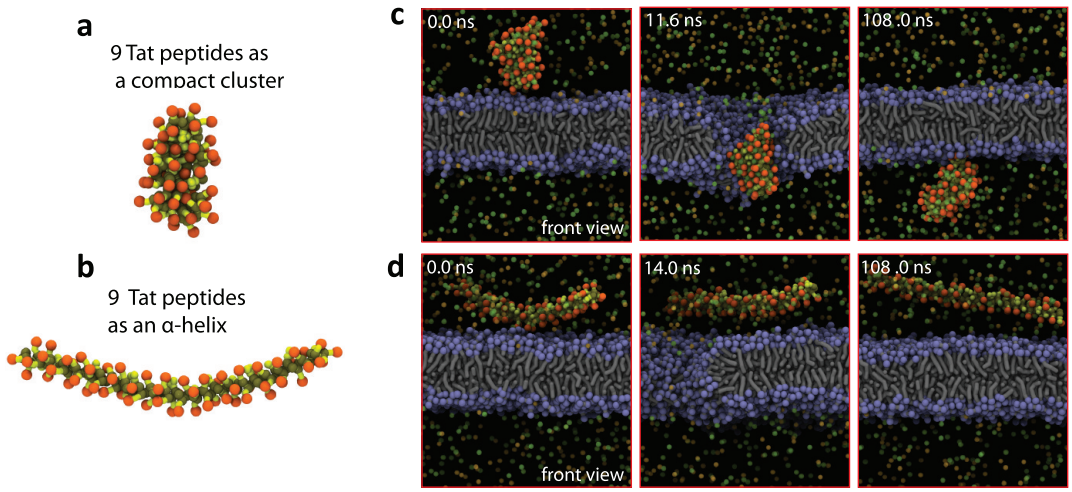

Figure 6. Effect of shape on the peptide translocation behavior. A compact cluster (a) and an α-helix (b) both comprising 9 Tat peptides are tested in the double-membrane system under −1.5 V TM potential. Snapshots (c, d) show different translocation behavior of the spheroidal cluster and the chain-like α-helix.

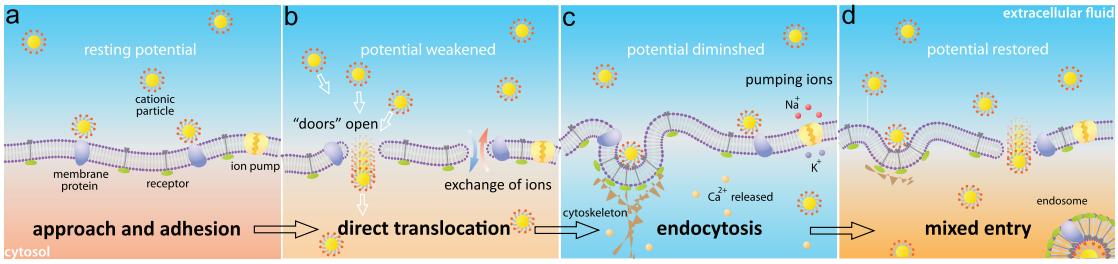

Figure 7. Uptake kinetics of cationic particles. (a) Cationic particles approach and adhere to negatively charged proteins on the cell membrane surface. (b) More particles diffuse close to the membranes and change the local electric field. Cell membranes open "doors" for particles, allowing them to directly translocate into the cytosol. (c) Transmembrane potential decreases and intracellular Ca^{2+} level increases. Cationic particles are taken up by the cell through receptor-mediated endocytosis. (d) Transmembrane potential is gradually restored. Uptake of cationic particles shows a mixed entry (direct translocation and endocytosis simultaneously).

transmembrane potential is depleted. Then the particles can no longer enter cells by this direct translocation mechanism. Instead, they enter cells by endocytosis (Figure 7c).[1] This stage corresponds to the slowing of the uptake process.[32] In response to the side effect of uptake, the depolarized cells will try to reestablish their inner potential by launching a series of cellular processes, including the increase of Ca^{2+} level in the cytosol. As the TM potential is gradually restored, some of the particles are able to enter the cell again by direct translocation, while others are taken up by the cell through endocytosis (Figure 7d). This corresponds to the slight recovery of the uptake process.[32] In principle, the uptake rate of direct translocation should depend on the restoration rate of the TM potential. However cellular response triggered by depolarization is an extremely complicated and dynamic process; thus more information is needed to understand the post-effect of initial uptake. Generally, one will always observe a mixed entry pathway of both direct translocation and endocytosis.

For the particles that cannot be pushed thought holes on living cell plasma membranes due to their shape or other factors that hinder their translocation, they are probably being pushed closer to the membrane surface by the electric field or even partly penetrate the holes, which eventually leads to the anchoring of the particles on the membranes (Figure S8). This will accelerate the subsequent endocytosis process as it increases the contract area between particles and the cell plasma membrane. Indeed, experiments have shown that even if it is not direct penetration, positively charged nanoparticles have a much faster rate of endocytosis.[2,32]

CONCLUSIONS

In summary, cationic NPs and CPPs can spontaneously translocate across model cell membranes under a TM potential through a similar mechanism. Transient holes are generated on the bilayer membrane in response to a strong local potential difference that serves to drive the particles inside the cell. Afterward, the membranes reseal themselves and the TM potential in the local area is diminished. The shape of the cationic particles greatly affects their translocation

behavior. Such membrane potential-driven translocation is also utilized by cationic agents to enter the cell nucleus (it is believed that the cell nucleus carries a further negative potential to the cytosol), which is why cationic agents are demonstrated to have a higher nuclear localization rate in various experiments.[36,37] Therefore, the TM potential not only is necessary in the regulation of various cell essential functions but also provides a natural avenue for cationic agents to enter cells. In fact, this intrinsic feature of cells may have been harnessed by certain proteins for their energy-independent entry, as some viruses have already evolved to utilize this natural weakness to break cell boundaries. Biomedical engineers could exploit this weakness in their favor in designing novel drug carriers and gene vectors.

METHODS SECTION

Polarizable Water in the CG Model. The MARTINI CG force field is used in our simulations.[38] The CG model is developed on the basis of structural properties of molecules and partitioning free energies in different solvents. Using a 4:1 mapping scheme, the model manages to enhance computational efficiency by roughly 3 orders of magnitude compared to atomistic models. Here we apply explicit polarizable water to give a relatively accurate description of the electrostatic interactions, however, at the expense of increasing computational cost.[27] The structure of the standard and polarizable water can be seen in Figure S1. The standard CG water does not have an explicit dipole momentum. Therefore the system is treated with a global dielectric constant of $\varepsilon_r = 15$, which is a compromise between large ε in water and small ε in the hydrophobic regions such as the interior of the lipid membrane. In the polarizable water model, the global dielectric constant is reduced to $\varepsilon_r = 25$ to give a realistic dielectric behavior in the hydrophobic regions.

CG Model of AuNPs. The gold nanocrystalline core of the gold nanoparticle is characterized by face-centered cubic (fcc) lattice structures and truncated-octahedron (TO) morphology.[39] It has a "magic number" of 314 with a diameter of 2.2 nm (Figure S2a). The core was obtained by cutting the TO+ crystal out of a bulk gold face-centered-cube lattice. Many-body embedded-atom potential was employed to equilibrate the core at room temperature.[40] We obtained the distribution of alkanethiol chains on the surface of the core by atomistic molecular dynamics simulation with various force fields in combination.[41] The final number of equilibrated alkanethiol chains on the bare Au_{314} core was 104, which yielded a coverage of 60.0% and surface area per thiol chain of 0.075 nm^2 (Figure S2b). The atomistic AuNP model is mapped into CG beads according to the MARTINI mapping scheme. After the mapping, we calibrated the bond and nonbond parameters between the beads in the CG force field to fit experimental data, which is the radius of gyration, diffusion coefficient, and average carbon distance (Figure S2d).[42]

CG Model of Tat Peptide. The HIV-1 Tat peptide has the residues YGRKKRRQRRR, which feature positively charged arginine and lysine groups. The CG model of the Tat peptides is built according to the newly added MARTINI protein force field. The new protein force fields are developed following the same philosophy as the lipid force field in MARTINI.[43] Figure S3 indicates the intra amino acid bonded potentials for different geometric classes of amino acids (containing either one, two, three, or four side-chain beads plus one backbone bead). The all-atomic model of the Tat peptide was generated with PEP-FOLD.[44] The atomistic model was then converted into the CG model according the MARTINI mapping scheme. The secondary structure of the Tat peptides is set to be a random coil. The CG Tat peptide was then relaxed in water. Figure S4 shows both the equilibrated atomistic structure and CG structure of a single Tat peptide.

Double-Membrane System. Dipalmitoylphosphaticylcholine is used as lipid molecules. Two patches of identical lipid membranes have a total of 2064 DPPC, and each membrane possesses 1032 lipid molecules. The dimensions of the system are 18 nm × 18 nm × 50 nm. The lower membrane is 5 nm away from the bottom of the box, while the upper membrane is 20 nm away from the top. After adding polarizable water solvent, the system was simulated for 40 ns to equilibrate the water and lipid membranes. Salt (NaCl) was introduced to the solvent at physiological concentration (150 mM), followed by another 40 ns simulation to equilibrate the ions. A typical simulation system in this article has a 30 ionic imbalance, which results in an approximately −1.5 V transmembrane potential ("intracellular region" relative to "extracellular region"). Figure S5 gives the charge density of both Na^+ and Cl^- in the double-membrane system.

Simulation Setup. Typically, nanoparticles/peptides are placed 3 nm above the upper membrane. After the insertion of the cationic objects, counterions are added to the solvent to ensure electroneutrality. Before the production run, nanoparticles/peptides as well as the two lipid membranes were constrained for another 10 ns to further equilibrate water and counterions. Periodic boundary conditions were applied. The system temperature was set at 305 K for all cases. Berendsen temperature coupling and Berendsen pressure coupling are used to set the system in an *NPT* ensemble. The particle mesh ewald (PME) method was applied to calculate the long-range electrostatic interactions. The dielectric constant is set at 2.5 to ensure realistic behavior of polarizable water. Short-ranged electrostatic interactions are cut off at 1.4 nm, while van de Waals interactions are cut off at 1.2 nm. All simulations were performed by the GROMACS 4.5.6 package.[45]

Conflict of Interest: The authors declare no competing financial interest.

Acknowledgment. This work was supported by the NSF through the NSF MRSEC program at MIT under grant no. DMR-0819762. Partial support from the MGHPCC is also greatly appreciated.

Supporting Information Available: Detailed information of the coarse-grained model and polarizable CG water (Figure S1), construction of the CG AuNPs (Figure S2) and CG HIV-1 Tat peptides (Figures S3 and S4), electric properties of the double-membrane system (Figures S5 and S6), concentration dependence of the HIV-1 Tat peptide on the translocation behavior (Figure S7), anchoring of Tat-AuNP complex on a model membrane (Figure S8), video example of direct translocation of a cationic AuNP across a model membrane (SV1), and video example of direct translocation of a 9 HIV-1 Tat peptide across a model membrane (SV2). This material is available free of charge *via* the Internet at http://pubs.acs.org.

REFERENCES AND NOTES

1. Doherty, G. J.; McMahon, H. T. Mechanisms of Endocytosis. *Annu. Rev. Biochem.* **2009**, *78*, 857–902.
2. Nativo, P.; Prior, I. A.; Brust, M. Uptake and Intracellular Fate of Surface-Modified Gold Nanoparticles. *ACS Nano* **2008**, *2*, 1639–1644.
3. Avrvizo, R. R.; Miranad, O. R.; Thompson, M. A.; Pabelick, C. M.; Bhattacharya, R.; Robertson, J. D.; Rotello, V. M.; Prakash, Y. S.; Mukherjee, P. Effect of Nanoparticles Surface Charge at the Plasma Membrane and Beyond. *Nano Lett.* **2010**, *10*, 2543–2548.
4. Chosh, P.; Han, G.; De, M.; Kim, C. K.; Rotello, V. M. Gold Nanoparticles in Delivery Applications. *Adv. Drug Delivery Rev.* **2008**, *60*, 1307–1315.
5. Sandhu, K. K.; McIntosh, C. M.; Simard, J. M.; Smith, S. W.; Rotello, V. M. Gold Nanoparticle-Mediated Transfection of Mammalian Cells. *Bioconjugate Chem.* **2002**, *13*, 3–6.

6. Lundberg, P.; Langel, U. A Brief Introduction to Cell-Penetrating Peptides. *J. Mol. Recognit.* **2003**, *16*, 227–233.
7. Torchilin, V. P.; Levchenko, T. S.; Rammohan, R.; Volodina, N.; Papahadjopoulos-Sternberg, B.; D'Souza, G. G. M. Cell Transfection *in Vitro* and *in Vivo* with Nontoixc TAT Peptide-Liposome-DNA Complexes. *Proc. Natl. Acad. Sci. U.S.A.* **2003**, *100*, 1972–1977.
8. Foged, C.; Nielsen, H. M. Cell-Penetrating Peptides for Drug Delivery across Membrane Barriers. *Expert Opin. Drug Delivery* **2008**, *5*, 105117.
9. Järver, P.; Langel, U. The Use of Cell-Penetrating Peptides as a Tool for Gene Regulation. *Drug Discovery Today* **2004**, *9*, 395–402.
10. Chen, J.; Hessler, J. A.; Putchakayala, K.; Panama, B. K.; Khan, D. P.; Hong, S.; Mullen, D. G.; DiMaggio, S. C.; Som, A.; Tew, G. N. Cationic Nanoparticles Induce Nanoscale Disruption in Living Cell Plasma Membranes. *J. Phys. Chem. B* **2009**, *113*, 11179–11185.
11. Leroueil, P. R.; Berry, S. A.; Duthie, K.; Han, G.; Rotello, V. M.; McNerny, D. Q.; Baker, J. R.; Orr, B. G.; Holl, M. M. Varieties of Cationic Nanoparticles Induce Defects in Supported Lipid Bilayers. *Nano Lett.* **2008**, *8*, 420–424.
12. Leroueil, P. R.; Hong, S.; Mecke, A.; Baker, J. R. J.; Orr, B. G.; Banaszak Holl, M. M. Nanoparticle Interaction with Biological Membranes: Does Nanotechnology Present a Janus Face?. *Acc. Chem. Res.* **2007**, *40*, 335–342.
13. Duchardt, F.; Fotin-Mleczek, M.; Schwarz, H.; Fischer, R.; Brock, R. A Comprehensive Model for the Cellular Uptake of Cationic Cell-Penetrating Peptides. *Traffic* **2007**, *8*, 848–866.
14. Marks, J. R.; Placone, J.; Hristova, K.; Wimley, W. C. Spontaneous Membrane-Translocating Peptides by Orthogonal High-Throughput Screening. *J. Am. Chem. Soc.* **2011**, *133*, 8995–9004.
15. Rothbard, J. B.; C., J. T.; Lewis, R. S.; Murray, B. A.; Wender, P. A. Role of Membrane Potential and Hydrogen Bonding in the Mechanism of Translocation of Guanidinium-Rich Peptides into Cells. *J. Am. Chem. Soc.* **2004**, *126*, 9506–9507.
16. Vives, E.; Brodin, P.; Lebleu, B. A Truncated HIV-1 Tat Brotein Basic Domain Rapidly Translocates through the Plasma Membrane and Accumulates in the Cell Nucleus. *J. Biol. Chem.* **1997**, *272*, 16010–16017.
17. Pouny, Y.; Rapaport, D.; Mor, A.; Nicolas, P.; Shai, Y. Interaction of Antimicobial Dermaseptin and Its Fluorescently Labeled Analogues with Phospholipid Membranes. *Biochemistry* **1992**, *31*, 12416–12423.
18. Gazit, E.; Lee, W. J.; Brey, P. T.; Shai, Y. Mode of Action of the Antibacterial Cecropin B2: A Spcetrofluorometric Study. *Biochemistry* **1994**, *33*, 10681–10692.
19. Van Lehn, R. C.; Alexander-Katz, A. Penetration of Lipid Bilayers by Nanoparticles with Environmentally-Responsive Surfaces: Simulations and Theory. *Soft Matter* **2011**, *7*, 11392–11404.
20. Lin, J. Q.; Zhang, H. W.; Chen, Z.; Zheng, Y. G. Penetration of Lipid Membranes by Gold Nanoparticles: Insights into Cellular Uptake, Cytotoxicity, and Their Relationship. *ACS Nano* **2010**, *4*, 3421–5429.
21. Reynwar, B. J.; Illya, G.; Harmandaris, V. A.; Müller, M. M.; Kremer, K.; Deserno, M. Aggregation and Vesiculation of Membrane Proteins by Curvature-Mediated Interactions. *Nature* **2007**, *447*, 461–463.
22. Herce, H. D.; Garcia, A. E. Molecular Dynamics Simulations Suggest a Mechanism for Translocation of the HIV-1 TAT Peptide across Lipid Membranes. *Proc. Natl. Acad. Sci. U.S. A.* **2007**, *104*, 20805–20810.
23. Ginzburg, V.; Balijepalli, S.; Smith, K.; Balazs, A. In *Nanotechnologies for the Life Sciences*; Kumar, C., Ed.; Wiley-VCH: 2009; Vol. 2.
24. Chen, X.; Tian, F.; Zhang, X.; Wang, W. Internalization Pathways of Nanoparticles and Their Interaction with a Vesicle. *Soft Matter* **2013**, *9*, 7592–7600.
25. Ginzburg, V. V.; Balijepalli, S. Modeling the Thermodynamics of the Interaction of Nanoparticles with Cell Membranes. *Nano Lett.* **2007**, *7*, 3716–3722.
26. Marrink, S. J.; Risselada, H. J.; Yefimov, S.; Tieleman, D. P.; De Vries, A. H. The MARTINI Force Field: Coarse Grained Model for Biomolecular Simulations. *J. Phys. Chem. B* **2007**, *111*, 7812–7824.
27. Yesylevskyy, S. O.; Schafer, L. V.; Sengupta, D.; Marrink, S. J. Polarizable Water Model for the Coarse-Grained MARTINI Force Field. *PLoS Comput. Biol.* **2010**, *6*, e1000810.
28. Tieleman, D. P.; Leontiadou, H.; Mark, A. E.; Marrink, S. J. Simulation of Pore Formation in Lipid Bilayers by Mechanical Stress and Electric Fields. *J. Am. Chem. Soc.* **2003**, *125*, 6382–6383.
29. Verma, A. U. O.; Hu, Y.; Hu, Y.; Han, H. S.; Watson, N.; Chen, S.; Irvine, D. J.; Stellacci, F. Surface-Structure-Regulated Cell-Membrane Penetration by Monolayer-Protected Nanoparticles. *Nat. Mater.* **2008**, *7*, 588–595.
30. Tatur, S.; Maccarini, M.; Barker, R.; Nelson, A.; Fragneto, G. Effect of Functionalized Gold Nanoparticles on Floating Lipid Bilayers. *Langmuir* **2013**, *29*, 6606–6614.
31. Van Lehn, R. C.; Atukorale, P. U.; Carney, R. P.; Yang, Y.-S.; Stellacci, F.; Irvine, D. J.; Alexander-Katz, A. Effect of Particle Diameter and Surface Composition on the Spontaneous Fusion of Monolayer-Protected Gold Nanoparticles with Lipid Bilayers. *Nano Lett.* **2013**, *13*, 4060–4067.
32. Cho, E. C.; Xie, J.; Wurm, P. A.; Xia, Y. Understanding the Role of Surface Charges in Cellular Adsorption *versus* Internalization by Selectively Removing Gold Nanoparticles on the Cell Surface with a I2/KI Etchant. *Nano Lett.* **2009**, *9*, 1080–1084.
33. Terrone, D.; Sang, S. L. W.; Roudaia, L.; Sivius, J. R. Penetratin and Related Cell-Penetrating Cationic Peptides Can Translocate across Lipid Bilayers in the Presence of a Transbilayer Potential. *Biochemistry* **2003**, *42*, 13787–13798.
34. Lee, H.; Larson, R. G. Multiscale Modeling of Dendrimers and Their Interactions with Bilayers and Polyelectrolytes. *Molecules* **2009**, *14*, 423–438.
35. Lee, H.; Larson, R. G. Lipid Bilayer Curvature and Pore Formation Induced by Charged Linear Polymers and Dendrimers: The Effect of Molecular Shape. *J. Phys. Chem. B* **2008**, *112*, 12279–12285.
36. Berry, C. C.; de la Fuente, J. M.; Mullin, M.; Chu, S. W. L.; Curtis, A. S. G. Nuclear Localization of HIV-1 Tat Functionalized Gold Nanoparticles. *IEEE Trans. Nanobioscience* **2007**, *6*, 262–269.
37. de la Fuente, J. M.; Berry, C. C. Tat Peptide as an Efficient Molecule to Translocate Gold Nanoparticles into the Cell Nucleus. *Bioconjugate Chem.* **2005**, *16*, 1176–1180.
38. Marrink, S. J.; de Vries, A. H.; Mark, A. E. Coarse Grained Model for Semiquantitative Lipid Simulations. *J. Phys. Chem. B* **2004**, *108*, 750–760.
39. Schmid, G.; Simon, U. Gold Nanoparticles: Assembly and Electrical Properties in 1−3 Dimensions. *Chem. Commun.* **2005**, *0*, 697–710.
40. Adams, J. B.; Foiles, S. M.; Wolfer, W. G. Self-Diffusion and Impurity Diffusion of fcc Metals Using the Five-Frequency Model and the Embedded Atom Method. *J. Mater. Res.* **1988**, *4*, 102–112.
41. Luedtke, W. D.; Landman, U. Structure and Thermodynamics of Self-Assembled Monolayers on Gold Nanocrystallites. *J. Phys. Chem. B* **1998**, *102*, 6566–6572.
42. Terrill, R. H.; Postlethwaite, T. A.; Chen, C. H.; Poon, C. D.; Terizis, A.; Chen, A.; Hutchison, J. E.; Clark, M. R.; Wignall, G. D.; Londono, J. D. Monolayer in Three Dimensions: NMR, SAXS, Thermal, and Electron Hopping Studies of Alkanethiol Stabilized Gold Clusters. *J. Am. Chem. Soc.* **1995**, *117*, 12537–12548.
43. Monticelli, L.; Kandasamy, S. K.; Periole, X.; Larson, R. G.; Tieleman, D. P.; Marrink, S. J. The MARTINI Coarse-Grained Force Field: Extension to Proteins. *J. Chem. Theory Comput.* **2008**, *4*, 819–834.
44. Thévenet, P.; Shen, Y.; Maupetit, J.; Guyon, F.; Derreumaux, P.; Tufféry, P. PEP-FOLD: An Updated de Novo Structure Prediction Server for Both Linear and Disulfide Bonded Cyclic Peptides. *Nucleic Acids Res.* **2012**, *40*, W288–W293.
45. Van Der Spoel, D.; Lindahl, E.; Hess, B.; Groenhof, G.; Mark, A. E.; Berendsen, H. J. C. GROMACS: Fast, Flexible and Free. *J. Comput. Chem.* **2005**, *26*, 1701–1718.